

## PLASMON RESONANCE AND RAMAN MODES IN Pb NANOPARTICLES OBTAINED IN EXTRACT OF *OPUNTIA FICUS-INDICA* PLANT

L. P. RAMÍREZ-RODRÍGUEZ\*, M. CORTEZ-VALADEZ\*<sup>§,¶</sup>,  
J.-G. BOCARANDO-CHACON<sup>†</sup>, H. ARIZPE-CHÁVEZ\*,  
M. FLORES-ACOSTA\*, S. VELUMANI<sup>‡</sup> and R. RAMÍREZ-BON<sup>§</sup>

\**Centro de Investigación en Física  
Universidad de Sonora. Apdo. Postal 5-88  
83190, Hermosillo, Son., México*

<sup>†</sup>*Universidad Tecnológica de Querétaro – UTEQ  
Avenida Pie de la Cuesta #2501, C. P. 76148  
Querétaro – Qro., México*

<sup>‡</sup>*Departamento de Ingeniería Eléctrica (SEES)  
Centro de Investigación y Estudios Avanzados del IPN  
Zacatenco, Av. IPN 2508, Col Zacatenco, D. F. 07360, México*

<sup>§</sup>*Centro de Investigación y Estudios Avanzados  
del IPN. Unidad Querétaro. Apdo. Postal 1-798  
76001, Querétaro, Qro., México*

<sup>¶</sup>*jcortez@qro.cinvestav.mx*

Received 11 December 2013

Accepted 20 May 2014

Published 20 June 2014

Colloidal nanoparticles were obtained by green synthesis, embedded in the *Opuntia ficus-indica* plant extract. Optical measurements allowed us to detect two absorption bands centered in 230 nm and 298 nm. Agglomerates of Pb nanoparticles have size in the range 2–8 nm. The effective absorption cross section of spherical Pb nanoparticles was calculated by applying the Mie theory for colloidal systems and compared to optical absorption measurements of Pb nanoparticles. The Raman spectrum of the samples after the reduction of Pb, shows a band at low wavenumbers centered at 116 cm<sup>-1</sup>. Similar bands have been assigned to small Pb and Ag clusters in other experimental results. Additionally, we used the density functional theory (DFT) as well as semi-empirical methods to assign this band to radial breathing modes of Pb metal nanoparticles.

*Keywords:* Pb nanoparticles; opuntia ficus-indica; DFT calculations; semi-empirical methods; Raman modes in nanoparticles.

## 1. Introduction

Simple and economic methods to obtain nanoparticles are viable alternative for reduction of costs in the technology of nanomaterials. Moreover, when eco-friendly chemical methods such as green synthesis are used, we reduce the environmental risks as hazardous chemicals avoided or are reduced. Use of the plant extract of *Opuntia ficus-indica* (*Ofi*) is suggestive because this plant has been found in more than 300 countries, and it has also the ability to survive in water scarcity and extreme weather conditions. Today, the plant has important applications in the treatment of contaminated water.

Applications of nanomaterials mainly depend on structural parameters such as size and morphology. These parameters are commonly quantified by microscopy techniques (such as scanning electron microscopy (SEM), transmission electron microscopy (TEM), etc). Nevertheless, relatively more accessible and simple techniques such as optical absorption have been employed for decades to estimate the reduction in size at the order of tens of nanometers of the material in neutral, cationic or anionic metallic clusters.<sup>1,2</sup> There are reports in literature on the formation and stabilization of colloidal Pb nanoparticles with size between 10 nm and 200 nm.<sup>3</sup> Recently, reports in spectroscopic prediction-detection of nanostructures by means of Raman studies have had remarkable contributions by our group, such as the detection of absorption bands in small metal clusters, and additional Raman bands in nanostructured oxides,<sup>4</sup> determined by the use of density functional theory (DFT) methods. In a recent work, we have obtained silver nanoparticles and found Raman bands at wavenumbers in the order of  $160\text{ cm}^{-1}$ , assigned to radial breathing modes in small silver nanoparticles.<sup>5</sup> The vibrational properties of small metal nanostructures have been measured in complex, extreme conditions such as ultra high vacuum and temperatures near 0 K.<sup>6</sup>

The aim of this work is to synthesize stable Pb nanoparticles by using a convenient green method as well as the theoretical and experimental description of their optical and vibrational properties. For this, Pb nanoparticles were stabilized in the extract of the plant *Ofi* at environmental conditions and their optical and vibrational properties were measured by optical and Raman spectroscopies. This provides an alternative to the study of vibrational and optical properties of various metal nanoparticles stabilized

in the extract of this plant. The size of the Pb nanoparticles was in the range 2–8 nm, as measured by TEM. Furthermore, this research includes DFT calculations in order to describe theoretically the breathing modes found in Pb nanoparticles. Also, the Mie theory was used to study the optical properties, as well as variations in the surface plasmon. The theoretical calculations by the DFT are limited to below 2 nm structures due to the computational cost. The Mie theory considered Pb nanoparticles with size in the range 1–5 nm. Since *Ofi* extracts show no Raman resonance at low wavenumbers, these plants offer a simple and inexpensive alternative to carry out analysis of vibrational frequencies of nanometric structures at low wavenumber.

## 2. Materials and Methods

To obtain the plant extract, a cactus pad from the main plant was cut in slices, and 25 g of these slices were mashed and added into 50 mL of deionized water. The mixture was left on constant magnetic stirring at room temperature for 30 min. After filtering, 3 mL of the solution were added into 25 mL of 0.001 M of aqueous solution of commercial lead nitrate ( $\text{Pb}(\text{NO}_3)_2$ ) and it was kept at 333 K for 1 h, in order to reduce the  $\text{Pb}^{2+}$  ions to Pb.

## 3. Results

The TEM image in Fig. 1(a) shows agglomerates of Pb nanoparticles with size between 2 nm and 8 nm, stabilized into the extract of *Ofi* plant. The particle size histogram in Fig. 1(b) shows that the average size of the nanoparticles is 4 nm. Additional energy dispersive X-ray spectroscopy (EDX) measurements confirm the presence of lead in these nanoparticles.

The exact mechanism of formation of metal nanoparticles using plants extracts remains a matter of debate in literature. Recent results indicate that formation of nanoparticles can take place in presence of colloidal starch<sup>7</sup> and, on the other hand, it is well known that ascorbic acid<sup>8</sup> stabilizes metal nanoparticles. Because the plant extract has a lot of ascorbic acid and starch, we assume that the proportions of these two kinds of molecules in the extract of *Ofi* play an important role in the reduction of lead ions and stabilization of lead nanoparticles.

Figure 2 shows the optical absorption spectrum produced by Pb colloidal nanoparticles in aqueous solution. Experimental data points were fitted

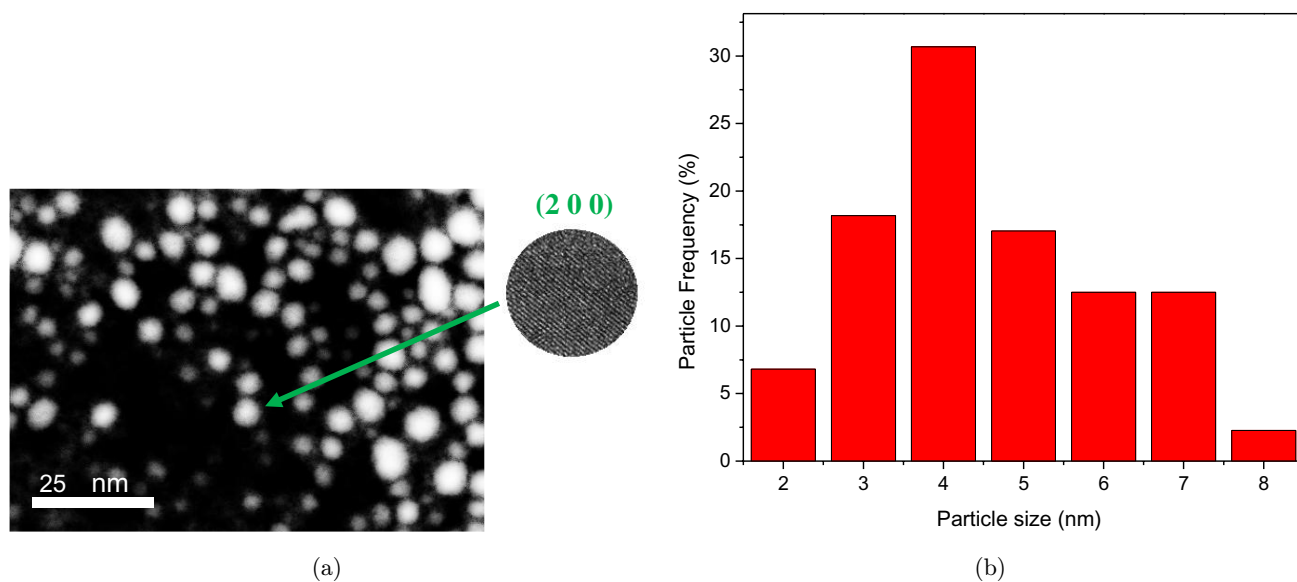


Fig. 1. (a) TEM images of the Pb nanoparticles synthesized in *Ofi* plant and (b) Particle size histogram.

with two Gaussian peaks that depict the absorption signal, and are centered about to 229 nm and 298 nm. It is well known that the absorption bands shown by nanostructures in the UV region show a shift caused by the particle size. Experimental results of Pb nanoparticles synthesized in zeolite matrix show an absorption band located in the UV region at 218 nm due to the surface plasmon in lead nanoparticles with size approximately to 10 nm.<sup>1</sup> In other experimental results, an absorption band of about 220 nm was observed, which was assigned to colloidal lead nanoparticles.<sup>9</sup> On the other hand,

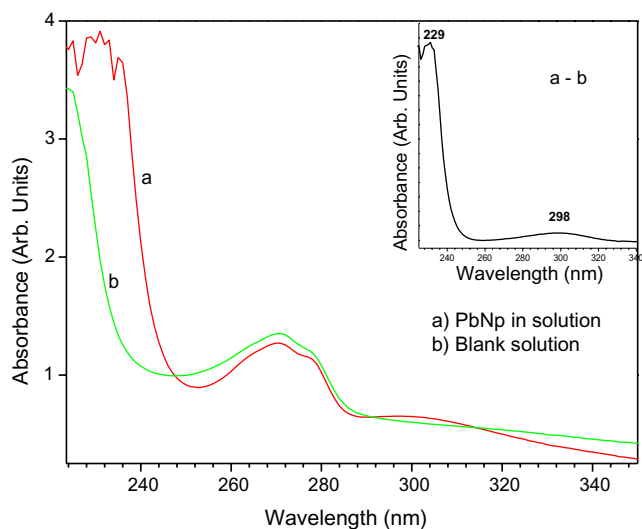


Fig. 2. Optical absorption spectra obtained experimentally of: (a) Pb nanoparticles in *Ofi* extract and (b) *Ofi* extract.

experimental studies found a band in 290 nm attributed to plasmon surface oscillations present in colloidal lead nanoparticles. The resonance at 290 nm has been reported by Henglein *et al.* in 1992.<sup>10</sup> We have studied the theoretical dipole resonance as a function of the particle radius,  $R$ , in the cases where  $1 \leq R \leq 5$  nm, considering reported experimental parameters and using the Mie theory predictively and complementary to our data. These results are shown in Fig. 3. Mie was the first to address the spreading of an electromagnetic wave due to a sphere of radius  $a$ .<sup>11</sup> Multipolar expansions

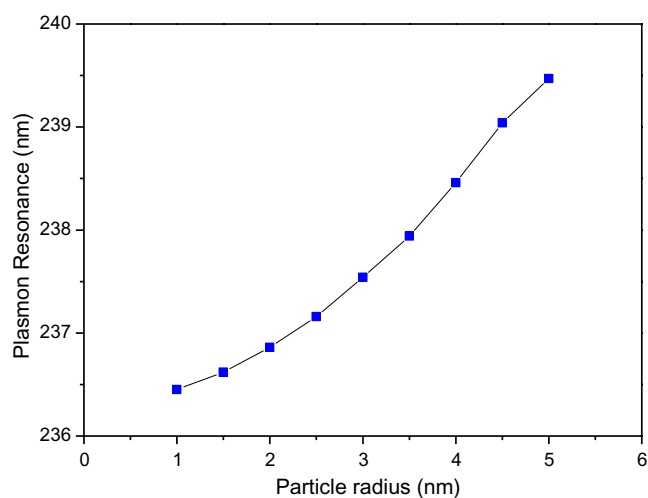


Fig. 3. Plasmon resonance relation with the particle radius, calculated by the Mie theory.

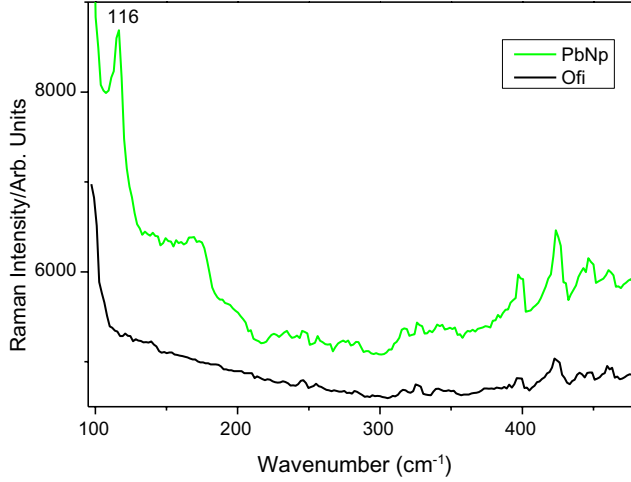


Fig. 4. Raman spectra of Pb-Ofi extract and Ofi extract samples.

describe the involved fields, as it is shown in the Eqs. (1) and (2).

$$\vec{E} = Z \sum_{l=1}^{\infty} \left\{ a_{lm} f_l(qr) \vec{X}_{lm}(\theta, \varphi) + \frac{ib_{lm}}{qr} [r f_l(qr)]' \hat{r} \right. \\ \left. \times \vec{X}_{lm}(\theta, \varphi) - \frac{b_{lm}}{q} \sqrt{l(l+1)} Y_{lm}(\theta, \varphi) \frac{f_l(qr)}{r} \hat{r} \right\}. \quad (1)$$

$$\vec{H} = \sum_{l=1}^{\infty} \left\{ b_{lm} f_l(qr) \vec{X}_{lm}(\theta, \varphi) - \frac{ia_{lm}}{qr} [r f_l(qr)]' \hat{r} \right. \\ \left. \times \vec{X}_{lm}(\theta, \varphi) + \frac{a_{lm}}{q} \sqrt{l(l+1)} Y_{lm}(\theta, \varphi) \frac{f_l(qr)}{r} \hat{r} \right\}. \quad (2)$$

The field inside the sphere is  $f_l(qr) = j_l(qr)$  and the scattered field is  $f_l(qr) = h_l^{(1)}(qr)$ ;  $q$  is the wave-number of the medium,  $Y_{lm}(\theta, \varphi)$  are the spherical harmonics  $y$   $\vec{X}_{lm} = \frac{1}{i\sqrt{l(l+1)}} \hat{r} \times \nabla Y_{lm}(\theta, \varphi)$  and  $Z$  is the impedance of the medium. Using the boundary conditions for the electromagnetic fields and the Poynting vector yields the extinction cross section.

$$\sigma_{\text{ext}} = \frac{1}{q_1^2} \sum \text{Re}(a_{i1}^s + b_{i1}^s). \quad (3)$$

Plasmons are identified by the relative maxima of the extinction cross section. Based on Mie theory and the Drude model, the variations of the surface plasmon relating to the particle radius were obtained. The values are given in Fig. 3. The optical properties of Pb were taken from Ref. 12, bulk

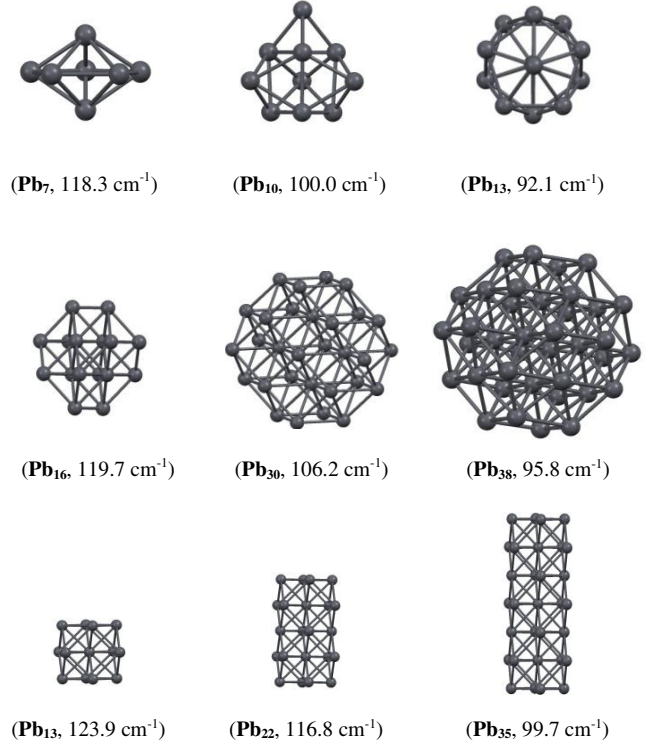


Fig. 5. A selection of particularly stable minima  $Pb_n$  clusters obtained by DFT ( $n = 7, 10, 13$ ) and selected fcc-like clusters by PM6 ( $n = 16, 30, 38, 13, 22$  and  $35$ ) ( $Pb_n$ , radial breathing mode).

plasma energy is 11.3 eV and the high-frequency dielectric constant is 1.1. The model predicts Plasmon resonance bands in the 236–240 nm range which agrees with the most intense band observed in Fig. 2 for Pb nanoparticles with 4 nm of average size.

The Raman spectrum of the extract, taken before and after the Pb reduction, was analyzed, and we found an additional Raman mode at low wavenumbers in the sample with lead content, as shown in Fig. 4. Although we have assigned similar Raman modes to amorphous Pb nanoparticles, we have now observed a high crystal symmetry shown by these agglomerates, as it is shown in Fig. 1. Currently we are carrying out theoretical studies to find an assignment to the Raman band present.

The DFT at the level of approximation Local Spin Density Approximation (LSDA) in combination with the Stuttgart/Dresden (SDD) basis set was used to study the Raman modes of some small clusters of Pb.

Theoretical calculations about vibrational properties in molecules and nanostructures predicted by the DFT usually represent a good agreement to experimental results.<sup>4,5</sup> Some particular cases have been studied with high stability previously

considered by Li *et al.* ( $\text{Pb}_n$ ,  $n = 7, 10, 13$ ).<sup>13</sup> A Raman mode with large relative intensity in each case, assigned to radial breathing modes by LSDA/SDD approximation level is present in these structures.

Additionally, when considering larger structures, we obtained radial breathing modes for spherical type form ( $\text{Pb}_n$ ,  $n = 16, 30, 38$ ) and cubic clusters ( $\text{Pb}_n$ ,  $n = 13, 22, 35$ ) both, with fcc-like geometry. These were studied by the semi-empirical PM6 method, due to the high level of approximation for crystalline solids of large size. All this are performed in order to theoretically consider structures similar to those found in Fig. 1.

Radial breathing modes with larger relative intensity in each case are present in clusters studied with both theories (Fig. 5). In Fig. 5, a clear shift to lower wavenumbers occurs in the position of the radial breathing mode when the size of the cluster increases, thus confirming no detection of Raman bands in spectroscopic studies of Pb-bulk. All calculations were performed using the software GAUSSIAN09.<sup>14</sup>

#### 4. Conclusion

These results show that the green synthesis of lead nanoparticles, by the use of the *Ofi* plant extract, is a fast, economic and environmental friendly method. In addition, this plant results are attractive for the study of optical and vibrational properties of small metal nanoparticles. We have observed that theoretical breathing radial modes are present in highly stable structures when DFT is used, and also in larger structures of the type fcc (less than 2 nm) when semi-empirical methods are used. These modes appear at low wavenumbers of about 90–120  $\text{cm}^{-1}$ . By extending this behavior to particles of few nanometers, we can assign the Raman band found at low wavenumbers in Fig. 4 to radial breathing modes of Pb nanoparticles synthesized in the *Ofi* plant extract.

#### Acknowledgments

The computational resources for this work were provided by UNISON/Acarus.

#### References

1. J. F. Román-Zamorano, M. Flores-Acosta, H. Arizpe-Chávez, F. F. Castellón-Barraza, M. H.

2. Farías and R. Ramírez-Bon, *J. Mater. Sci.* **44**, 4781 (2009).
3. L. L. A. Adams, W. R. Sweeney and H. M. Jaeger, *J. Phys. Chem. C* **114**, 6304 (2010).
4. M. Veith *et al.*, *Comptes Rendus Chimie* **7**, 509 (2004).
5. M. Cortez-Valadez, A. Vargas-Ortiz, L. Rojas-Blanco, H. Arizpe-Chávez, M. Flores-Acosta and R. Ramírez-Bon, *Physica E* **53**, 146 (2013).
6. J.-G. Bocarando-Chacon, M. Cortez-Valadez, D. Vargas-Vazquez, F. R. Melgarejo, M. Flores-Acosta, P. G. Mani-Gonzalez, E. Leon-Sarabia, A. Navarro-Badilla and R. Ramírez-Bon, *Physica E* **59**, 15 (2014).
7. H. Sontag, B. Eberle and R. Weber, *Chem. Phys.* **80**, 279 (1983).
8. N. Vigneshwaran, R. P. Nachane, R. H. Balasubramanya and P. V. Varadarajan, *Carbohydr. Res.* **341**, 2012 (2006).
9. L. Wang, C. Hu, Y. Nemoto, Y. Tateyama and Y. Yamauchi, *Cryst. Growth Des.* **10**, 3454 (2010).
10. A. Henglein, P. Mulvaney, A. Holzwarth, T. E. Sosebee, A. Fojtik and Ber. Bunsen-Ges, *Phys. Chem.* **96**, 754 (1992).
11. A. Henglein, E. Janata and A. Fojtik, *J. Phys. Chem.* **96**, 4734 (1992).
12. G. Mie, *Ann. Phys.* **330**, 377 (1908).
13. P. Mulvaney, *Langmuir* **12**, 788 (1996).
14. X.-P. Li, W.-C. Lu, Q.-J. Zang, G.-J. Chen, C. Z. Wang and K. M. Ho, *J. Phys. Chem. A* **113**, 6217 (2009).
15. M. J. Frisch, G. W. Trucks, H. B. Schlegel, G. E. Scuseria, M. A. Robb, J. R. Cheeseman, G. Scalmani, V. Barone, B. Mennucci, G. A. Petersson, H. Nakatsuji, M. Caricato, X. Li, H. P. Hratchian, A. F. Izmaylov, J. Bloino, G. Zheng, J. L. Sonnenberg, M. Hada, M. Ehara, K. Toyota, R. Fukuda, J. Hasegawa, M. Ishida, T. Nakajima, Y. Honda, O. Kitao, H. Nakai, T. Vreven, J. A. Montgomery, Jr., J. E. Peralta, F. Ogliaro, M. Bearpark, J. J. Heyd, E. Brothers, K. N. Kudin, V. N. Staroverov, T. Keith, R. Kobayashi, J. Normand, K. Raghavachari, A. Rendell, J. C. Burant, S. S. Iyengar, J. Tomasi, M. Cossi, N. Rega, J. M. Millam, M. Klene, J. E. Knox, J. B. Cross, V. Bakken, C. Adamo, J. Jaramillo, R. Gomperts, R. E. Stratmann, O. Yazzev, A. J. Austin, R. Cammi, C. Pomelli, J. W. Ochterski, R. L. Martin, K. Morokuma, V. G. Zakrzewski, G. A. Voth, P. Salvador, J. J. Dannenberg, S. Dapprich, A. D. Daniels, O. Farkas, J. B. Foresman, J. V. Ortiz, J. Cioslowski and D. J. Fox, Gaussian 09 (Revision B.01), Gaussian, Inc., Wallingford CT, 2010.